HEFAT2008
6th International Conference on Heat Transfer, Fluid Mechanics and Thermodynamics
30 June to 2 July 2008
Pretoria, South Africa
Paper number: MO1

OPTIMAL MIXING OF MULTIPLE REACTING JETS IN A GAS TURBINE COMBUSTOR

J.P. Meyer*, O.S. Motsamai, and J.A. Snyman
*Author for correspondence
Department of Mechanical & Aeronautical Engineering
University of Pretoria, Pretoria 0002, South Africa
E-mail address: jmeyer@up.ac.za
Tel: 0027 12 420 31046, Fax: 0027 12 362 5124

ABSTRACT
This paper addresses the design optimisation methodology used to optimise a gas turbine combustor exit temperature profile. The methodology uses computational fluid dynamics and mathematical optimisation to optimise the combustor exit temperature profile. The studies from which the results were derived, investigated geometric variations of a complex three-dimensional flow field in a gas turbine combustor. The variation of geometric parameters impacts on mixing effectiveness, of which the combustor exit temperature profile is a function. The combustor in this study is an experimental liquid-fuelled atmospheric combustor with a turbulent diffusion flame. The computational fluid dynamics simulations use the Fluent code with a standard k-ε model. The optimisation is carried out with the Dynamic-Q algorithm, which is specifically designed to handle constrained problems where the objective and constraint functions are expensive to evaluate. All the optimisation cases investigated led to an improved combustor exit temperature profile as compared to the original one.

I. INTRODUCTION
The desire to continuously improve the performance and working life of aircraft gas turbine engines has led to the need for more advanced engine hardware that is capable of surviving in very intense flow and thermal environments. Improvements in engine performance come in the form of increasing thrust production while increasing the working life of the individual engine components. Increasing the thrust can be accomplished by increasing the gas working temperature of the turbine section [1,2]. As a result of the push for higher temperatures, the temperatures of gas exiting combustors of modern engines are well above the melting point of the metal alloys of the engine components [1]. This also puts a lot of pressure on the development of blade cooling technologies. It would be a losing battle if the focus of research is only directed at material and blade cooling technologies. Therefore, the designers should also address the characteristics of the gases exiting the combustor. The fact that the combustor exit temperature has a drastic effect on the life of turbine blades, and hence the maintenance costs, makes it a critical design consideration.

A general methodology for design optimisation of the combustor exit temperature profile, is presented here. The methodology is considered for application during detailed design of the combustor as opposed to preliminary design. The methodology combines CFD and mathematical optimisation [3] to flatten the combustor exit temperature profile, by varying geometric parameters. Thus the design parameters become optimisation variables, and performance trends are optimised with respect to these variables by an appropriate optimisation algorithm. This approach can be better described as design-by-analysis and optimisation.

NOMENCLATURE

f	mixture fraction
$f(\boldsymbol{x})$	objective function
$g_j(\boldsymbol{x})$	j-th inequality constraint function
$h_j(\boldsymbol{x})$	k-th equality constraint function
R^n	n-dimensional real space
T	temperature
T_{max}	maximum temperature at the combustor exit
$\boldsymbol{x}$	design vector

Sub-/Superscripts

i	inlet
o	outlet
i,j,k	index

II. NUMERICAL TOOL FOR FLOW ANALYSIS
A. Geometric Model
The configuration considered in this study is a can-type atmospheric combustor (Fig. 1) developed by Morris [4] for combustion research. The combustor has ten curved (45°) swirler passages, six primary holes, 12 secondary holes and ten dilution holes. The combustor has a length of 174.8 mm and a diameter of 82.4 mm. The fuel nozzle is modelled from experimental data with a discrete drop model. This research

combustor was used as a preliminary design model, and as a basis for the optimisation study. Since the configuration is symmetrical, only half of the geometry was modelled. Due to the complexity of the geometry and automation required by the optimisation method, the physical domain has been discretised using an unstructured tetrahedral mesh. It was found from a sensitivity study that 500 000 computational cells provided an adequate compromise between accuracy and speed.

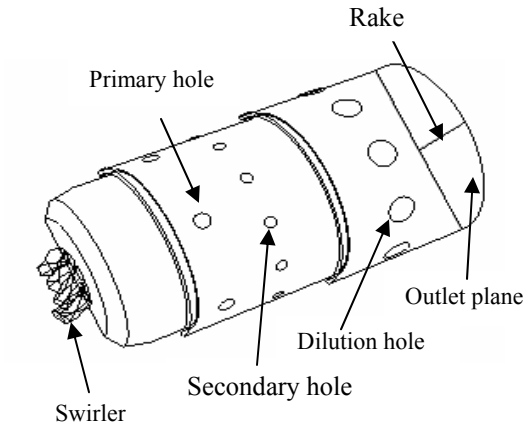

Figure 1. Three dimensional model of the combustor

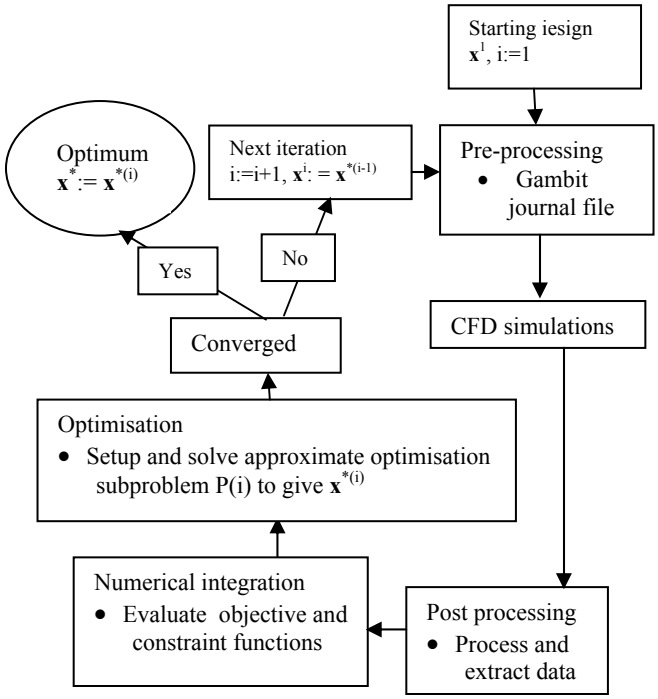

Figure 2. Flow diagram of FLUENT coupled to optimiser

Since geometric modelling and grid generation are the most time-consuming and labour-intensive processes in CFD-based design systems, the GAMBIT journaling toolkit has been intensively used to repeat model building for different CFD sessions. The procedures were written in parametric form, such that when a variation of a particular analysis case is generated, one only needs to change the value in the parameter file, and then re-run the procedures. A flow diagram of the iterative optimisation procedure is shown in Fig. 2. For every iteration or given starting design $\boldsymbol{x}^i$, i=1,2,3…, the mathematical optimiser generates a new set of variables that needs to be evaluated. A journal file is then generated with the current variables and passed to GAMBIT to generate the mesh used in FLUENT. After the CFD simulation has converged, a file is written to a hard disk that is then processed to derive the data that will be processed with the numerical integrating code to yield the objective function. The mathematical optimiser obtains all the data, sets up a new approximate optimisation subproblem *P(i),* and computes the associated new optimum design $\boldsymbol{x}^{*(i)}$. For the next iteration $i:=i+1$ the new starting design is set at $\boldsymbol{x}^{(i)}:=\boldsymbol{x}^{*(i-1)}$ and the new subproblem is constructed and solved. This process is repeated until convergence to the global optimum $\boldsymbol{x}^*$ is obtained. With this implementation, the time required to generate an improved geometry has been reduced from the order of days to minutes.

B. Boundary Conditions

Boundary conditions that need to be specified are the mass flow inlets through the swirler, primary holes, secondary holes and dilution holes. The combustor outlet plane is modelled as a pressure outlet boundary. The symmetry boundary planes are modelled as rotational periodic boundary conditions. The air flow distribution boundary conditions were obtained from measurements [4]. The total mass flow rate of air in to the combustor is 0.1 kg/s. The mass flow splits are as follows: 8.4% through the swirler, 12.5% through the primary holes, 15.3% through the secondary holes and 60.5% through the dilution holes.

The fuel spray model is characterised by a minimum diameter of 5.8 μm, a Sauter mean diameter (SMD) of 27.37 μm, a maximum drop size of 204 μm, drop size parameter (X) = 38 μm and a drop size spread parameter of 1.78. The droplets were divided into 16 different size ranges and are introduced into the combustor at 36 discrete circumferential injection points equally spaced at the centre of the combustor. The non-atomiser model used, involves building a cone. A cone was constructed for 5, 12, 19, 26, 32, and 40 degrees. The injection velocity for all droplets was 32.5 m/s.

C. Computational Approach

The commercial software developed by Fluent Inc [5] was used to perform the numerical analyses of the study. The selected pre-processor, GAMBIT, acts both as a geometry modeller and mesh generator. The CFD code solves the gas equations in Eulerian form whereas the droplets are treated in a Lagrangian formulation with discrete trajectories. Turbulence was modelled using the standard k-ε model along with wall functions for the treatment of the near-wall regions.

The standard k-ε model has limitations in capturing regions of strong stream-wise curvatures, as well as vortices and boundary layer separation. However, the model is computationally inexpensive and that makes it ideal for this design optimisation study. This is necessitated by the fact that the work involves many CFD simulations that take long to converge. To reduce the computational effort, the following further simplifications have been implemented: the effects of buoyancy forces have been neglected so that only a periodic portion of the domain is analysed, the pressure variations are so small that the flow has been considered incompressible, and due to the fact that this is an atmospheric combustor, whereby soot particles will be small in diameter, radiation has also been neglected [2].

For the mixture fraction/PDFmodel a PDF file was generated with a Pre-PDF processor. The PDF file was imported into Fluent to set up the Fluent case file. The PDF file contains a look-up table needed by the mixture fraction/PDF model. The equilibrium mixture calculated by the PDF model was assumed to consist of nine different species and radicals: $C_{13}H_{24}$, CO_2, N_2, O_2, H_2O, CO, H_2, O, and OH.

III. COMBUSTOR NUMERICAL FLOW FIELDS

The CFD results for the velocity vectors in the longitudinal planar section at the symmetry plane of the combustor are shown in Fig. 3. The plots display the swirling flow, the primary, and the secondary and dilution penetration. The primary zone is located between the swirlers and primary holes. The recirculation zone in the combustor primary zone is caused by the joint effect of the primary jet impingement and shearing, upstream of the jet. The mixing and recirculation in this zone provide an ideal aerodynamic condition for evaporation of the fuel spray and ignition of the mixture. Satisfactory combustion is achieved when the spray is enclosed in the swirling recirculation zone. Actually, the swirling recirculation is designed to induce combustion products to flow upstream to meet and merge with the incoming fuel and air. This action also assists in stabilising the flame. When sprays are trapped in recirculation zones, droplets are sufficiently mixed with the high temperature gas, heated by the surrounding area and vaporised, and finally react with the air. Otherwise, the combustion is incomplete due to the poor distribution and mixing.

For the current study, the central toroidal recirculation zone (CTRZ) shifted slightly off-axis near the location of the primary jet injection and may not trap all the spray droplets. According to Durbin *et al*. [6], this is a sign of low swirl. The presence of a corner recirculation zone (CRZ) is also a sign of low swirl and when swirl is high, the corner recirculation zone becomes negligible. A carefully controlled primary flow field creates an on-axis toroidal recirculation zone, unlike in the current case where the on-axis toroidal recirculation zone has not been achieved. Due to the lack of optimised flow fields, a non-uniform combustor exit temperature profile (Fig. 4) has resulted, and in order to get a uniform combustor exit temperature profile the combustor flow fields must be carefully controlled (optimised).

The pattern factor $\left(T_{\max} - T_o\right) / \left(T_o - T_i\right)$ in Fig. 4 is 0.5, and it is the temperature traverse quality. The pattern factor can be used to assess how good the mixing at the exit of the combustor is.

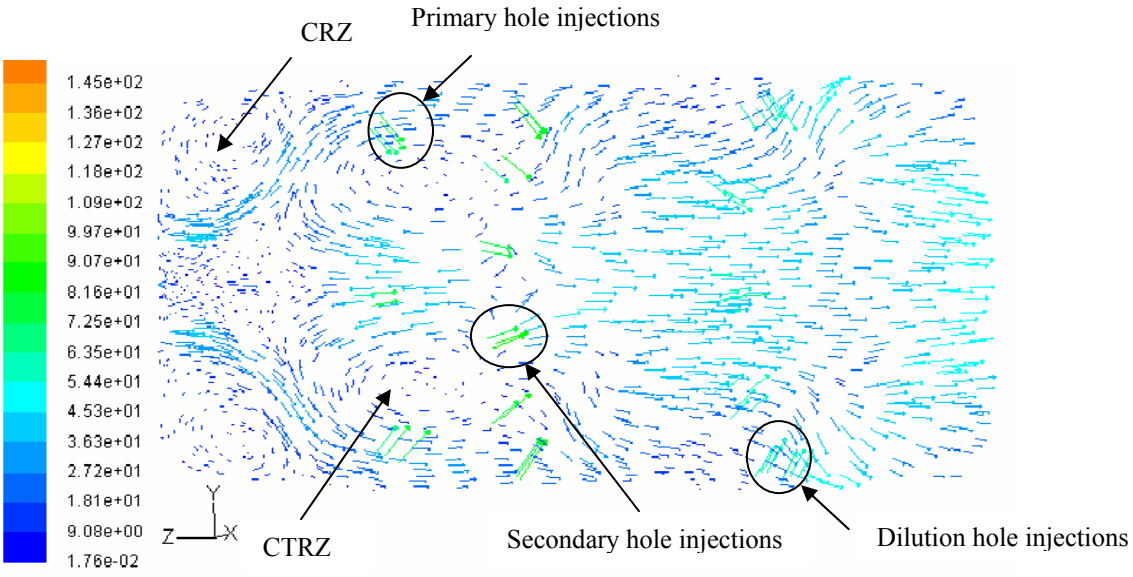

Figure 3. Flow field on the symmetry plane of the combustor

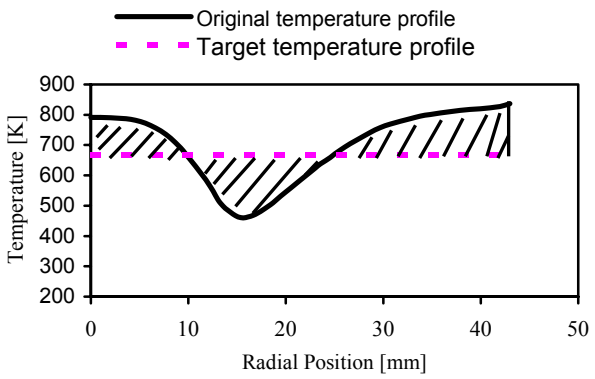

Figure 4. Non-optimized combustor exit temperature profile

IV. MATHEMATICAL OPTIMIZATION

Computational fluid dynamics has become an alternative tool for assessing different combustor designs. As an optimisation tool, however, it has limitations in that the variation of many parameters is necessary and trial-and-error simulations, are required of which the interpretation relies heavily on the insight of the modeller. For combustor applications, numerical optimisation can be used after the preliminary design phase and during detailed design as part of the fine-tuning process. The preliminary design uses empirical and semi-empirical tools to achieve design tasks quickly [7]. After the preliminary design phase, most of the combustor requirements are fixed and critically analysed in order to perform a first comparison between achievements and targets.

The main advantage of mathematical optimisation is that the designer is unburdened from the trial-and-error process by the use of an optimisation algorithm, requiring no human interaction. The designer can focus on the formulation of the design objectives and the analysis (post-processing) of the optimisation results. In addition, mathematical optimisation may lead to unexpected designs and thus to new design philosophies.

Consider the constrained optimisation problem of the general mathematical form:

$$\min\ f(\mathbf{x});\ \mathbf{x}=\left[x_1,x_2,...,x_i,...,x_n\right]^T,\ \mathbf{x}\in R^n \qquad (1)$$

subject to constraints:

$$\begin{aligned} g_j(\mathbf{x}) &\le 0;\ \ j=1,2,...,m \\ h_k(\mathbf{x}) &= 0;\ \ k=1,2,...,p<n \end{aligned} \qquad (2)$$

where $f(\mathbf{x})$, $g_j(\mathbf{x})$ and $h_k(\mathbf{x})$ are scalar functions of the n-dimensional vector $\mathbf{x}$.

The function $f(\mathbf{x})$ is the objective function that is being minimised. The $g_j(\mathbf{x})$ denote the inequality constraint functions and $h_k(\mathbf{x})$ the equality constraint functions. The components x_i, i=1,2,…,n of $\mathbf{x}$ are called the design variables.

The optimum vector $\mathbf{x}$ that solves the above problem is denoted by $\mathbf{x}^*$:

$$\mathbf{x}^*=\left[x_1^*,x_2^*,...,x_n^*\right]^T \qquad (3)$$

The optimisation problem formulated in (1)-(2) may be solved using many different gradient-based methods, such as the successive approximation sequential quadratic programming (SQP) method, or stochastic methods such as genetic algorithms. Genetic algorithms are often found to be too expensive in terms of the number of function evaluations (simulations) when compared with SQP [8,9]. The method of choice for the work done here is the relatively new gradient-based and successive approximation Dynamic-Q method [3].

Dynamic-Q [3] involves the application of the dynamic trajectory method (LFOP) for unconstrained optimization, which is adapted to handle constrained problems through an appropriate penalty function formulation [10]. In Dynamic-Q the dynamic trajectory method is applied to successive approximate spherically quadratic subproblems of the original problem constructed from appropriate sampling of the objective and constraint functions and their gradients. Here use is made of finite forward differencing to obtain gradients of the objective and constraint functions, which implies that n + 1 simulations are required per design optimisation iteration. The method also employs a fixed move limit on each variable to improve the convergence.

The Dynamic-Q algorithm can be summarised as follows (see Fig. 2) [3]:

1. Choose a starting point $\mathbf{x}^1$ and move limits δ_j, $j:=1,2,...,n$ and set $i:=1$.
2. Evaluate $f(\mathbf{x}^i)$, $g_j(\mathbf{x}^i)$ and $h_j(\mathbf{x}^i)$ as well as gradient vectors $\nabla f(\mathbf{x}^i)$, $\nabla g_j(\mathbf{x}^i)$ and $\nabla h_j(\mathbf{x}^i)$. If termination criteria are satisfied then set $\mathbf{x}^*:=\mathbf{x}^i$ and stop.
3. Construct a local approximate subproblem $P[i]$ at $\mathbf{x}^i$ using appropriate spherically quadratic approximations to the objective and constraints functions [3].
4. Solve the approximate subproblem $P[i]$ to give $\mathbf{x}^{*i}$ by using LFOPC [10].

5. Set $i := i + 1$, $\mathbf{x}^i := \mathbf{x}^{*(i-1)}$ and return to Step 2.

V. OPTIMISATION PROBLEMS

A. Two design variables (Case 1)

This case considers the widely used approach of optimising combustor exit temperature profile by selecting dilution hole parameters as design variables [2], specifically, the number of dilution holes and the diameter of dilution holes. The number of dilution holes were allowed to vary between two and seven and the diameter between four and eight. Therefore, the limits are set as $2 \le x_1 \le 7$ and $4 \le x_2 \le 8$, where x_1 = number of dilution holes and x_2 = diameter of dilution holes. The explicit optimisation problem is therefore:

Minimise $f(\mathbf{x})$ = Shaded Area in Fig. 4
such that: x_1 an integer, $x_2 \in R$

The original combustor exit temperature profile in Fig. 4, was generated with initial (starting) values of $x_1 = 5$ and $x_2 = 6$. The move limits for x_1 and x_2 are 2 and 1 respectively, and the perturbation sizes for calculating gradients are 1 and 0.4. No explicit inequality or equality constraints have been used, so that the minimum found is essentially for an unconstrained problem, although limits have been set on design variables so as to ensure that the problem remains realistic. The integer solutions were selected by the rounding off of the continuous approximate solutions obtained.

B. Five design variables (Case 2)

In this case, five design variables are considered for design optimisation and the variables are: the radius of primary holes (x_1), number of primary holes (x_2), number of dilution holes (x_3), radius of dilution holes (x_4) and swirler angle (x_5). The primary hole parameters and swirler angle are considered because the recirculation zone has a tremendous effect on combustion of which the combustor exit temperature profile is a result. The optimisation parameters for Case 2 are given on Table 1.

An inequality constraint is imposed so that the pressure drop does not exceed the initial pressure drop by 8% ($\Delta p \le 160$ Pa). The formulation of the optimisation problem is now as follows:

Minimise $f(\mathbf{x})$ = Shaded Area in Fig. 4
such that:

$$g_1 = \Delta p - 160 \le 0 \quad \text{(inequality constraint)}$$

$$g_j = -x_j + x_j^{\min} \le 0, \quad j = 1, 2, ..., 5$$

$$g_{j+2} = x_j - x_j^{\max} \le 0, \quad j = 1, 2, ..., 5$$

where $x_j^{\min}$ and $x_j^{\max}$ denote the upper and lower limits on the variation of the variables. In addition, move limits (see Table 1) are also imposed.

Here x_2, x_3 are integers, and x_1, x_4, $\in$ R

Table 1. Optimisation parameters for Case 2

	x_1	x_2	x_3	x_4	x_5
Initial values	3.3	3	5	6	45
Move limits	0.4	2	2	1	0.5
Perturbations sizes	0.2	1	1	0.4	1
Lower limit	2.3	2	2	4	45
Upper limit	2.9	6	7	8	65

VI. SIMULATION AND OPTIMISATION RESULTS

The results obtained from both the CFD simulations and optimisation runs are discussed in this section. Figure 5 shows the target exit temperature profile and the original exit temperature profile for the non-optimized case. The two curves differ considerably in shape. According to Morris [4], it is because the flow splits were not optimised during the preliminary design.

A. Two design variables (Case 1)

The optimised combustor exit temperature profile is shown in Fig. 5 for Case 1, where two variables are used. In this figure the corresponding target and non-optimised combustor exit temperature profiles are also shown. A comparison of the non-optimised and the optimised combustor exit temperature profiles shows an improvement, because the severe sinusoidal nature of the non-optimised (original) combustor exit temperature profile has been lessened. The pattern factor was 0.50 before design optimisation and 0.36 after design optimisation, showing some improvement.

Figure 6 shows the optimisation history of the objective function. The objective function essentially levels out after seven design iterations, showing that the objective function has converged. The objective function has apparently converged to a local optimum, with the global optimum for this case probably corresponding to the lower value (F=4.8) of the objective function reached at iteration six (see Fig. 6). The objective function has decreased from 5.3 to 4.8 at iteration six, which represents a decrease of 9.4% and corresponds to a feasible design. At this minimum value of the objective function, the design variables are given as $x_1 = 4$ (number of dilution holes), and $x_2 = 4$ (diameter of dilution holes) as shown in Fig. 7. It can be observed in Fig. 7 that the design variables are still changing after the eighth iteration, although the objective function in Fig. 6 has levelled off. This indicates that the last three designs in the optimisation run are effectively equivalent

having the same objective function value (shaded area between the two curves in Fig. 4), although the design variables differ slightly.

Figure 8 shows the exit temperature contours on the centre plane (left side) and outlet plane (right side) of the combustor for both non-optimised (Fig. 8a) case and optimised (Fig. 8b) case. The exit temperature contours in Fig. 8b are better than in Fig. 8a. In Fig. 8a, there is a hot section in the centre and a cold section mid-way, and a variation of cold and hot sections close to the wall of the combustor. This is caused by poor mixing due to the non-optimised number and diameter of dilution jets. The mixing is significantly improved in Fig. 8b. The left sides of Fig. 8a and Fig. 8b show how the jet penetrates the combustor. It can be noticed that the jet in Fig. 8a under-penetrates, whereas the one in Fig. 8b penetrates deeper into the combustor causing an improvement in mixing. The pattern factor for Case 1 has improved from 0.50 (Fig. 4) to 0.36 (Fig. 5) and this has the possibility of prolonging the life of the turbine blades.

In Case 1, the pressure drop has increased by 37% from the original value, which is an undesirable feature, though it is beneficial to combustion and dilution processes. This is because a high pressure drop results in high injection air velocities, steep penetration angles, and a high level of turbulence, which promotes good mixing [2]. These results show that the optimum design creates a higher pressure drop in the combustor, and therefore, it would be impossible for the design to be improved without using other design parameters without increasing pressure drop. Due to the fact that high pressure loss was experienced in Case 1, a pressure loss constraint was imposed in Case 2.

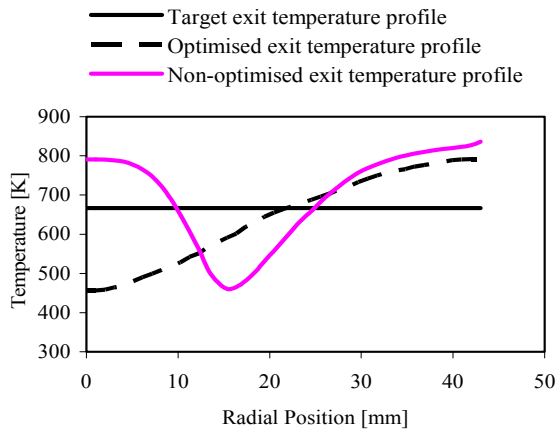

Figure 5. Optimised combustor exit temperature profile for Case1, which is two design variables (number of dilution holes and diameter of dilution holes)

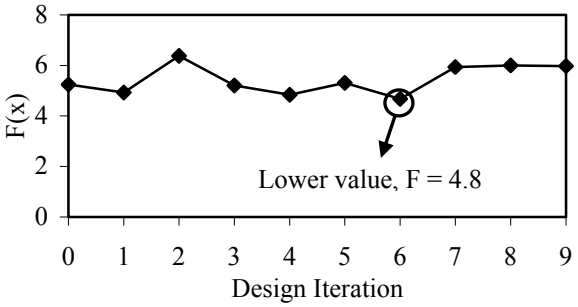

Figure 6. Optimisation history of the objective function for Case 1

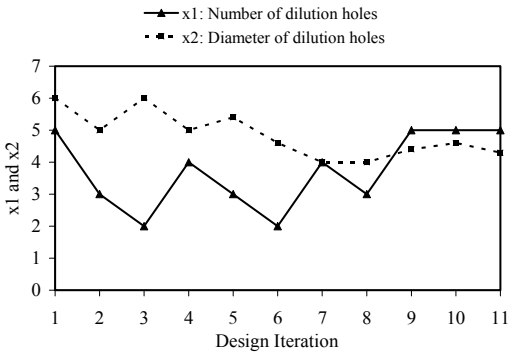

Figure 7. Optimisation history of design variables for Case 1

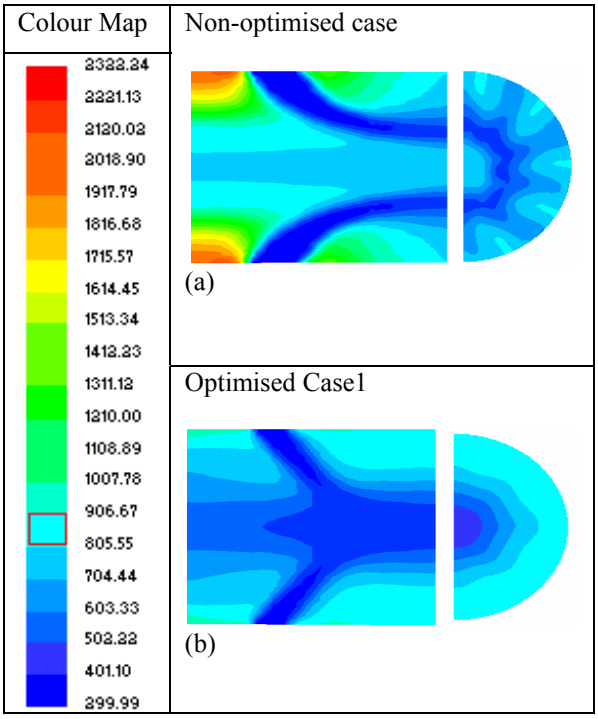

Figure 8. Temperature contours on the centre plane (left side) and exit (right side) of the combustor (a) for the non-optimised and (b) the optimized Case 1

B. Five design variables (Case 2)

The optimised combustor exit temperature profile for Case 2 with five design variables is shown in Fig. 9. In this figure the corresponding target and non-optimised combustor exit temperatures are also shown. A comparison of the non-optimised and the optimised combustor exit temperature shows an improvement, because the optimised combustor exit temperature profile is more uniform than the original exit temperature profile. Although the combustor exit temperature profile is improved by optimisation, the pattern factor has increased from 0.50 to 0.55.

Figure 10 shows the optimisation history of the objective function. It can be noticed that the objective function essentially levels out after nine design iterations, showing that the objective function has converged to a local minimum. Again the objective function has probably reached the neighborhood of the global minimum at iteration eight where it attains the value of 3.9, representing a decrease of 26% relative to its initial value of 5.3. At this minimum objective function value, the design is feasible (with g_1=-26 in Fig. 11) with variables given as x_1 = 3.9 (diameter of primary holes), x_2 = 2 (number of primary holes), x_3 = 3 (number of dilution holes), x_4 = 4.3 (diameter of dilution holes) and x_5 = 47.3° (swirler angle) as shown in Fig. 12. In Fig. 12, it can be observed that some design variables are still changing (though with small magnitudes) after the ninth iteration, although the objective function has almost levelled off. This indicates that the last three designs in the optimization run are effectively equivalent having almost the same objective function values (shaded area between the two curves in Fig. 4), although their geometries differ slightly.

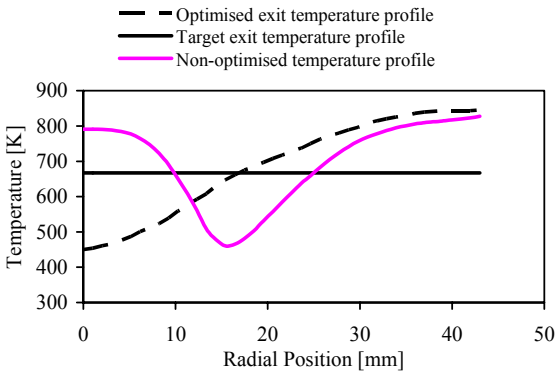

Figure 9. Optimised combustor exit temperature profile for Case 2

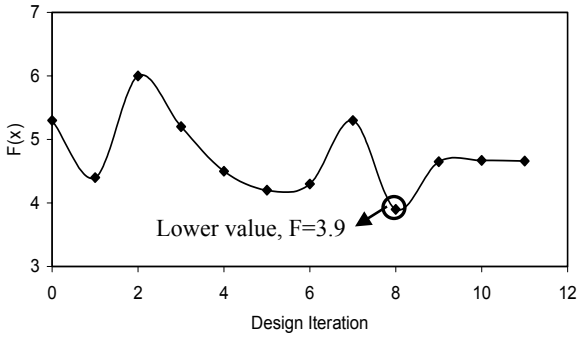

Figure 10. Optimisation history of the objective function for Case 2

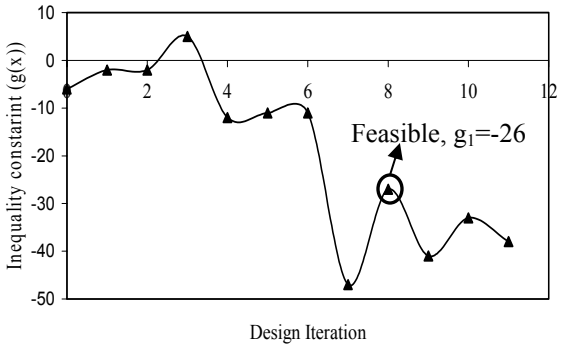

Figure 11. Optimisation history of design variables for Case 2

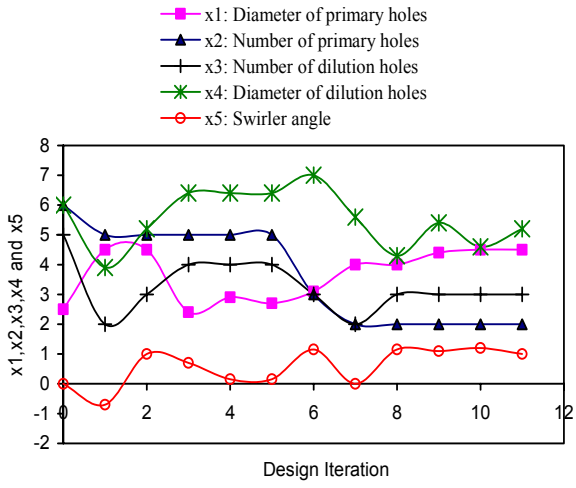

Figure 12. Optimisation history of inequality constraint (pressure drop) for Case 2

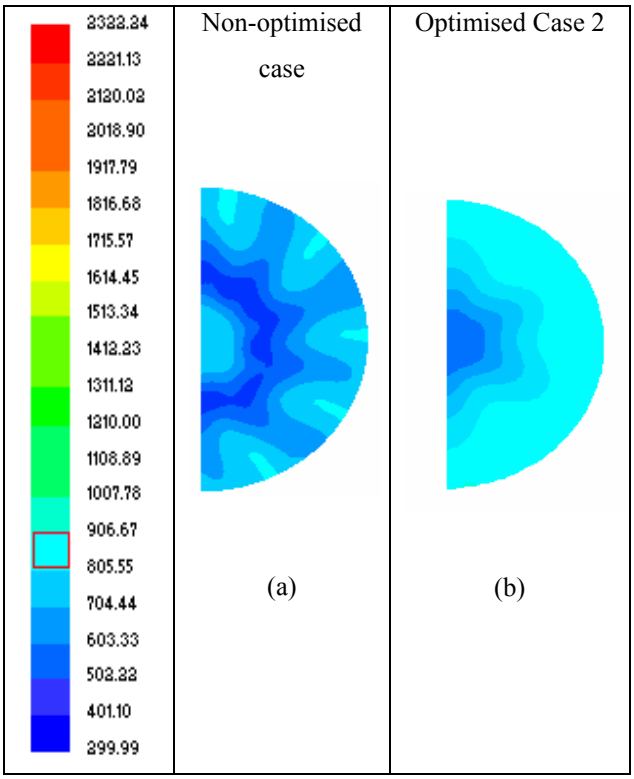

Figure 13. Temperature contours of the combustor exit plane for (a) the non-optimised and (b) the optimised for Case 2, with five design variables

Figure 13 shows the temperature contours of the combustor exit plane for both the non-optimised and the optimised cases. The combustor exit temperature contours in Fig. 13b are better than in Fig. 13a. In Fig 13a, there is a hot section in the centre and a cold section midway and a variation of cold and hot sections close to the wall of the combustor. This is caused by poor mixing due to an unoptimised flow field, which is improved in Fig. 13b.

VII. CONCLUSION

This paper has shown that CFD and mathematical optimisation can successfully be combined in gas turbine combustor design optimisation. The methodology was used to obtain a more uniform combustor exit temperature profile by optimising the combustor with two dilution hole variables for Case 1 and five design variables (for dilution holes and secondary holes) for Case 2. Increasing design variables from two (Case 1) to five (Case 2) provided optimum results that fell within acceptable limits of pressure drop. The optimiser returns a significant modification in the combustor exit temperature profile. The optimisation process was started with an extremely non-uniform combustor exit temperature profile, however, improved results were achieved for both cases. The methodology can be considered a supporting tool in the detailed design, complementing physical understanding as well as trial-and-error design.

It should be noted that this methodology cannot replace the empirical and semi-empirical design tools for preliminary design, but it is very useful when optimising the final design, to achieve certain performance requirements. Although the method was applied here to the combustor exit temperature profile it can possibly also be used for other performance measures as long as the objective function and constraints can be written as analytical or numerically approximated expressions. Future work will focus on incorporating the influence of other geometric parameters, to be used as design variables. The current results have not been validated against experimental results, but the proposed strategy was initially tested on a base case design example, on which model validation was performed with a well researched Berl Combustor [11] before this work was carried out, in order to cultivate the ability to reproduce correct reacting flow results. Confidence in the results of this work was derived from the base case design optimisation.

VIII. ACKNOWLEDGEMENTS

The authors wish to acknowledge the contributions of Prof J. A. Visser and Mr R. M. Morris to this study (formerly University of Pretoria colleagues).

IX. REFERENCES

1. Mongia, H. C., "A Synopsis of Gas Turbine Combustor Design Methodology Evolution of Last 25 Years," *Proceedings of ISABE,* 2001-1086, 2001.
2. Lefebvre, A. H., *Gas Turbine Combustion*, 2nd Edition, Talylor & Fancis, Phiadelphia, 1998, p. 340.
3. Snyman, J. A., and Hay, A. M., "The Dynamic-Q Optimization Method: An Alternative to SQP?," *Computers and Mathematics with Applications*,Vol. 44, No. 12, 2002, pp. 1589-1598.
4. Morris, R. M., "An Experimental and Numerical Investigation of Gas Turbine Research Combustor," MSc. Dissertation, University of Pretoria, 2000.
5. FLUENT, Software package, Ver. 6.2.16, Fluent Inc., Lebanon, NH, 2004.
6. Durbin, M. D., Vangsness, M. D., Balla, D. R., and Katta, V. R., "Study of Flame Stability in a Step Swirl Combustor," *ASME paper 95-GT-111*, 1995.

7. Mongia, H. C., "Aero-thermal Design and Analysis of gas Turbine Combustion Systems: Current Status and Future direction," *AIAA paper 98-3982*, 1998.
8. Baumal, A. E., McPhee, J. and Calamai, P. H., "Application of genetic algorithms of an active vehicle suspension design," *Computer Methods in Applied Mechanics and Engineering*," Vol. 163, 1998, pp. 87-94.
9. Eberhard, P., Schiehlen, W., and Bestle, D., "Some advantages of stochastic methods in multi-criteria optimization of multibody systems," *Archive of Applied Mechanics,* Vol. 69, 1998, pp. 543-554.
10. Snyman, J. A., "The LFOPC Leap-Frog Algorithm for Constrained Optimization," *Computers and Mathematics with Applications*, Vol. 40, 2000, pp. 1085-1096.
11. Motsamai, O. S., Visser, J. A., Morris, R. M., and De Kock, D. J., "Validation Case for Multi-Disciplinary Design Optimisation of a Combustor," *Proceedings of Botswana Institution of Engineers - Power and Renewable Energy*, Botswana, 2005, pp. 19-21.